Cell

Structural Basis for RNA Unwinding by the DEAD-Box Protein *Drosophila* Vasa

Toru Sengoku,[1,2] Osamu Nureki,[1,6] Akira Nakamura,[3] Satoru Kobayashi,[4] and Shigeyuki Yokoyama[1,2,5,*]
[1] Department of Biophysics and Biochemistry, Graduate School of Science, University of Tokyo, 7-3-1 Hongo, Bunkyo-ku, Tokyo 113-0033, Japan
[2] RIKEN Genomic Sciences Center, 1-7-22 Suehiro-cho, Tsurumi, Yokohama 230-0045, Japan
[3] Center for Developmental Biology, RIKEN, 2-2-3 Minatojima-Minamimachi, Chuou-ku, Kobe, Hyogo 650-0047, Japan
[4] Center for Integrative Bioscience, Okazaki National Research Institutes, 38 Nishigonaka, Myodaiji, Okazaki, Aichi 444-8585, Japan
[5] RIKEN SPring-8 Center, Harima Institute, 1-1-1 Kouto, Sayo, Hyogo 679-5148, Japan
[6] Present address: Department of Biological Information, Graduate School of Bioscience and Biotechnology, Tokyo Institute of Technology, 4259 Nagatsuta-cho, Midori-ku, Yokohama 226-8501, Japan.
*Contact: yokoyama@biochem.s.u-tokyo.ac.jp
DOI 10.1016/j.cell.2006.01.054

SUMMARY

DEAD-box RNA helicases, which regulate various processes involving RNA, have two RecA-like domains as a catalytic core to alter higher-order RNA structures. We determined the 2.2 Å resolution structure of the core of the *Drosophila* DEAD-box protein Vasa in complex with a single-stranded RNA and an ATP analog. The ATP analog intensively interacts with both of the domains, thereby bringing them into the closed form, with many interdomain interactions of conserved residues. The bound RNA is sharply bent, avoiding a clash with a conserved α helix in the N-terminal domain. This "wedge" helix should disrupt base pairs by bending one of the strands when a duplex is bound. Mutational analyses indicated that the interdomain interactions couple ATP hydrolysis to RNA unwinding, probably through fine positioning of the duplex relative to the wedge helix. This mechanism, which differs from those for canonical translocating helicases, may enable the targeted modulation of intricate RNA structures.

INTRODUCTION

Higher-order structures of RNA are formed by intramolecular and intermolecular base pairs and are important for their functions. RNA helicases regulate various cellular processes involving RNAs by catalyzing the alteration of higher-order RNA structures, such as secondary-structure melting, strand separation (Luking et al., 1998), and RNA-protein dissociation (Fairman et al., 2004; Jankowsky et al., 2001). The structural rearrangements are coupled to ATP binding and hydrolysis. DEAD-box proteins, which were named after the strictly conserved sequence Asp-Glu-Ala-Asp (D-E-A-D), are widely found from bacteria to human and constitute by far the largest RNA helicase family (Linder et al., 1989). The DEAD-box proteins are involved in many aspects of RNA metabolism, such as transcription, splicing, transport, translation, and degradation of mRNA and ribosome biogenesis (Rocak and Linder, 2004). So far, 26 DEAD-box protein-coding genes have been identified in the yeast genome, and most of them are essential for viability (de la Cruz et al., 1999).

The DEAD-box family belongs to helicase superfamily II (SF2), the largest helicase superfamily, which also includes the DEAH-box and Snf2 families (Gorbalenya and Koonin, 1993). In the SF2 proteins, the core consists of two tandemly repeated RecA-like domains, with motifs I, Ia, Ib, II, and III in the N-terminal RecA-like domain (NTD) and motifs IV, V, and VI in the C-terminal domain (CTD) (Caruthers and McKay, 2002). The DEAD sequence is located in motif II. Subsequent studies identified three additional motifs that are characteristic of the DEAD-box proteins (the Q and GG motifs in the NTD and the QxxR motif in the CTD) (Caruthers et al., 2000; Caruthers and McKay, 2002; Cordin et al., 2004; Svitkin et al., 2001; Tanner et al., 2003). Thus far, the structures of several DEAD-box proteins have been solved (Benz et al., 1999; Carmel and Matthews, 2004; Caruthers et al., 2000; Cheng et al., 2005; Johnson and McKay, 1999; Kurimoto et al., 2005; Shi et al., 2004; Story et al., 2001; Zhao et al., 2004). In these structures, the NTD and the CTD each conserve their folds, but the interdomain orientations are strikingly diverse. Motifs I and II in the NTD bind ATP or ADP (Benz et al., 1999; Shi et al., 2004), whereas motif VI in the CTD is believed to participate in the binding of ATP, although it is located too far from the NTD to collaboratively bind ATP in these structures.

A prototype of the DEAD-box proteins is the eukaryotic translation initiation factor 4A (eIF4A), which melts the secondary structures in the 5′UTR of mRNA and thereby facilitates ribosome scanning (Gingras et al., 1999). It

Table 1. Crystallographic Statistics

Data Collection					
Data set	Native	Se peak	Se edge	Se remote1	Se remote2
Wavelength (Å)	0.9120	0.9794	0.9796	0.9840	0.9710
Resolution (Å)[a]	50–2.20 (2.24–2.20)	50–2.40 (2.44–2.40)	50–3.00 (3.11–3.00)	50–3.00 (3.11–3.00)	50–3.00 (3.11–3.00)
Observations	321,846	583,066	148,849	150,949	145,347
Unique reflections	117,511	101,785	51,457	50,427	50,777
Completeness (%)[a]	89.6 (74.6)	97.5 (78.1)	95.6 (88.6)	96.8 (91.9)	95.5 (88.5)
Mean I/σ[a]	16.8 (2.2)	8.0 (1.6)	8.6 (2.8)	9.0 (3.2)	8.7 (2.9)
R_{merge} (%)[a,b]	7.5 (30.5)	15.3 (45.4)	11.3 (25.5)	11.9 (23.6)	10.7 (24.8)
Phasing					
Phasing power iso/ano		0.83/1.06	0.50/0.36	–/0.05	0.40/0.47
Figure of merit		0.39			
Refinement					
Resolution (Å)	R_{free} (%)	R_{work} (%)	Rmsd bond (Å)	Rmsd angle (°)	
50–2.20	25.0	19.7	0.00845	1.45	

[a] Numbers in parentheses correspond to the highest resolution shell.
[b] $R_{merge} = \Sigma_j|I_j - \langle I\rangle|/\Sigma I_j$, where I_j is the intensity of the jth reflection and $\langle I\rangle$ is the average intensity.

consists only of the tandem RecA-like domains, or the "helicase core." First, eIF4A was shown to unwind 5′- or 3′-tailed RNA duplexes in the presence of another translation initiation factor, eIF4B (Rozen et al., 1990). Later, it was found that eIF4A by itself can unwind short RNA duplexes (Rogers et al., 1999) and blunt-ended duplexes (Rogers et al., 2001). However, eIF4A does not unwind a long stretch of duplex (Rogers et al., 1999). These biochemical characteristics are quite different from those of other well-studied SF2 proteins. For example, hepatitis C virus NS3, an SF2 protein that unwinds both DNA and RNA, "processively" unwinds a long stretch of duplex and requires a single-stranded "loading strand" on the 3′ side of the substrate (Pang et al., 2002). In the mechanistic models of these helicases, the tandem RecA-like domains are proposed to work in concert with other auxiliary domains: The RecA-like domains act as a "motor" to translocate the bound single-stranded nucleic acid, while the auxiliary domain (or domains) acts as a "wedge" by providing steric hindrance with the other strand. Therefore, it is unlikely that the same model is applicable to the DEAD-box proteins. Clues to the unwinding mechanism of the DEAD-box proteins have been provided by mutant studies. The motif II DEAD-to-DEAH mutation and another mutation in motif III of eIF4A impaired the RNA unwinding activity but did not reduce the RNA binding and ATPase activities (Pause and Sonenberg, 1992). Nevertheless, how the DEAD-box proteins couple ATP hydrolysis to RNA unwinding and how this coupling is impaired in the mutants remained compelling questions.

Drosophila melanogaster Vasa is essential for development (Hay et al., 1988; Lasko and Ashburner, 1988). In the developing embryo, Vasa is localized in polar granules, and, through its interaction with eIF5B (Carrera et al., 2000; Johnstone and Lasko, 2004), it positively regulates the translation of specific mRNAs to produce protein factors required for embryonic patterning and germline differentiation (Breitwieser et al., 1996; Carrera et al., 2000; Markussen et al., 1997; Styhler et al., 1998; Tinker et al., 1998). Vasa homologs are specifically expressed in the germlines of higher eukaryotes, including human (Raz, 2000). An uncoupling between ATP hydrolysis and RNA unwinding was observed for the protein product of one mutant allele of *D. melanogaster vasa*, vas^{D5}, which has a mutation in motif V (Liang et al., 1994).

In the present study, we solved the crystal structure of the helicase-core region of Vasa bound with a single-stranded RNA (ssRNA) and AMPPNP, a nonhydrolyzable analog of ATP, at 2.2 Å resolution. In the structure, which represents the ATP bound closed form, the two RecA-like domains closely interact with each other and form the functional ATPase site. The two domains also interact with the bound RNA. The NTD induces a sharp bend on the 3′ side of the RNA by providing steric hindrance with an α helix. Conserved residues form interaction networks at the ATPase and RNA binding sites, which are important for coupling ATP hydrolysis to RNA unwinding. On the basis of these results, we propose a model for RNA unwinding by DEAD-box proteins.

RESULTS

Overall Structure of the Vasa-RNA Complex

The Vasa protein fragment (residues 200–623), containing the helicase core, was prepared, and the complex with

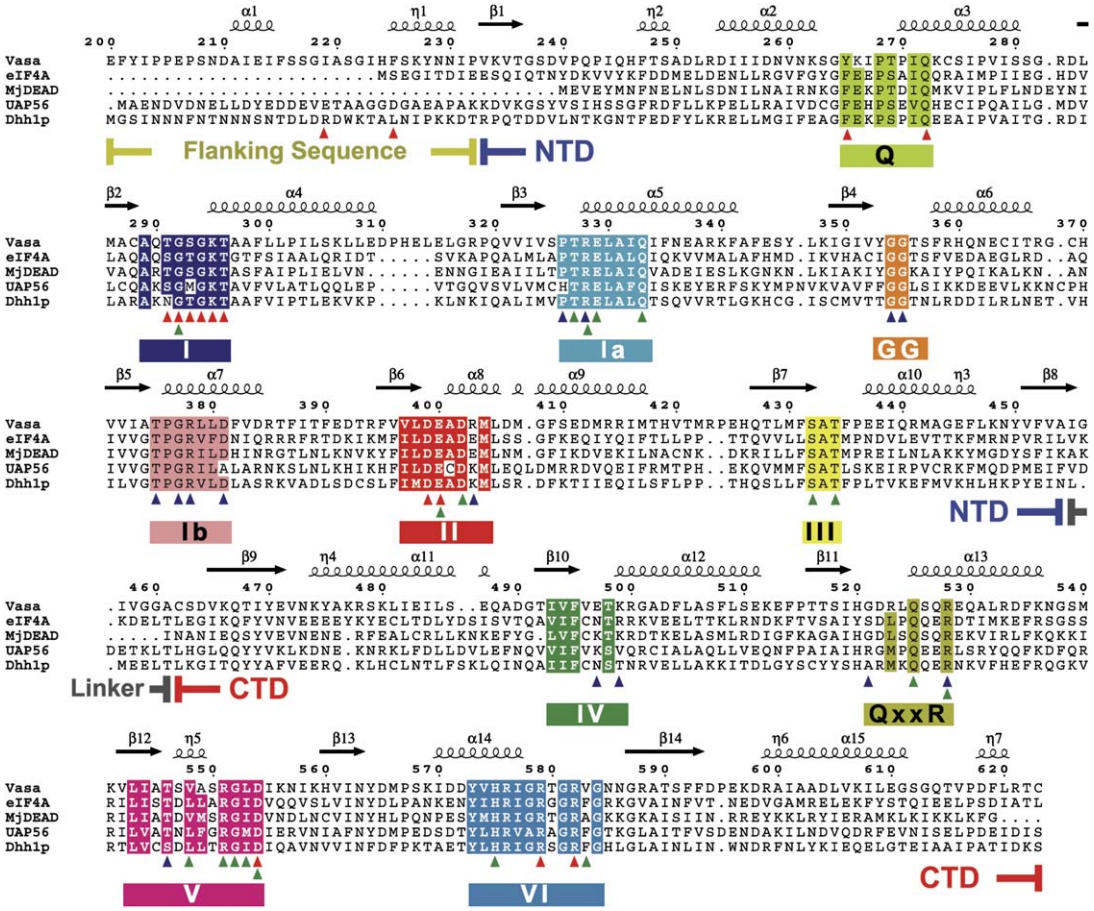

Figure 1. Sequence Alignment of DEAD-Box Proteins, Including Vasa

Red, blue, and green triangles indicate the residues involved in ATP binding, RNA binding, and interdomain interactions, respectively. Unless otherwise stated, color codes representing the motifs are used similarly in the other figures.

synthetic poly(U) RNA (U_{10}) and AMPPNP was crystallized (Sengoku et al., 2004). The crystal structure of the complex was determined at 2.2 Å resolution by the multiwavelength anomalous dispersion method using a selenomethionine-substituted protein (Table 1; see also Figure S1 in the Supplemental Data available with this article online). The final model contains residues 202–621 of Vasa, seven uridine residues, one AMPPNP molecule, and one Mg^{2+} ion per complex. The four independent complexes in the crystallographic asymmetric unit are essentially the same (pairwise root-mean-square deviations of 0.24–0.37 Å over all modeled α-carbons).

The protein can be divided into four regions: the flanking sequence (residues 202–232), the N-terminal domain (NTD; residues 233–454), the linker region (residues 455–462), and the C-terminal domain (CTD; residues 463–621) (Figure 1 and Figure 2A). The folds of these two domains are essentially the same as those of the other DEAD-box proteins. The flanking sequence, which is unique to the Vasa and Ded1p orthologs, runs halfway around the two RecA-like domains along the interdomain cleft. Residues 616–618, which are important for eIF5B binding (Johnstone and Lasko, 2004), are located at the C terminus of the CTD and are far from the conserved motifs (Figure 2B).

The relative orientation of the two domains in the present Vasa structure significantly differs from those in the other helicase-core structures of DEAD-box proteins, eIF4A, MjDEAD, UAP56, and Dhh1p (Caruthers et al., 2000; Cheng et al., 2005; Shi et al., 2004; Story et al., 2001). In the Vasa structure, the closely arranged NTD and CTD embed the AMPPNP in a deep interdomain cleft and interact with the RNA running perpendicular to the cleft (Figures 2A and 2B). In terms of the interdomain cleft, the Vasa structure is "closed," whereas all of the other structures are much more "open" (Figure 2C). The interdomain interactions in the Vasa structure are totally different from and more extensive than those in the MjDEAD, UAP56, and Dhh1p structures (Cheng et al., 2005; Shi et al., 2004; Story et al., 2001). Furthermore, the two domains of eIF4A are completely separated and form a "dumbbell" structure (Caruthers et al., 2000). Such domain rearrangements are due to conformational changes in the 8-residue linker

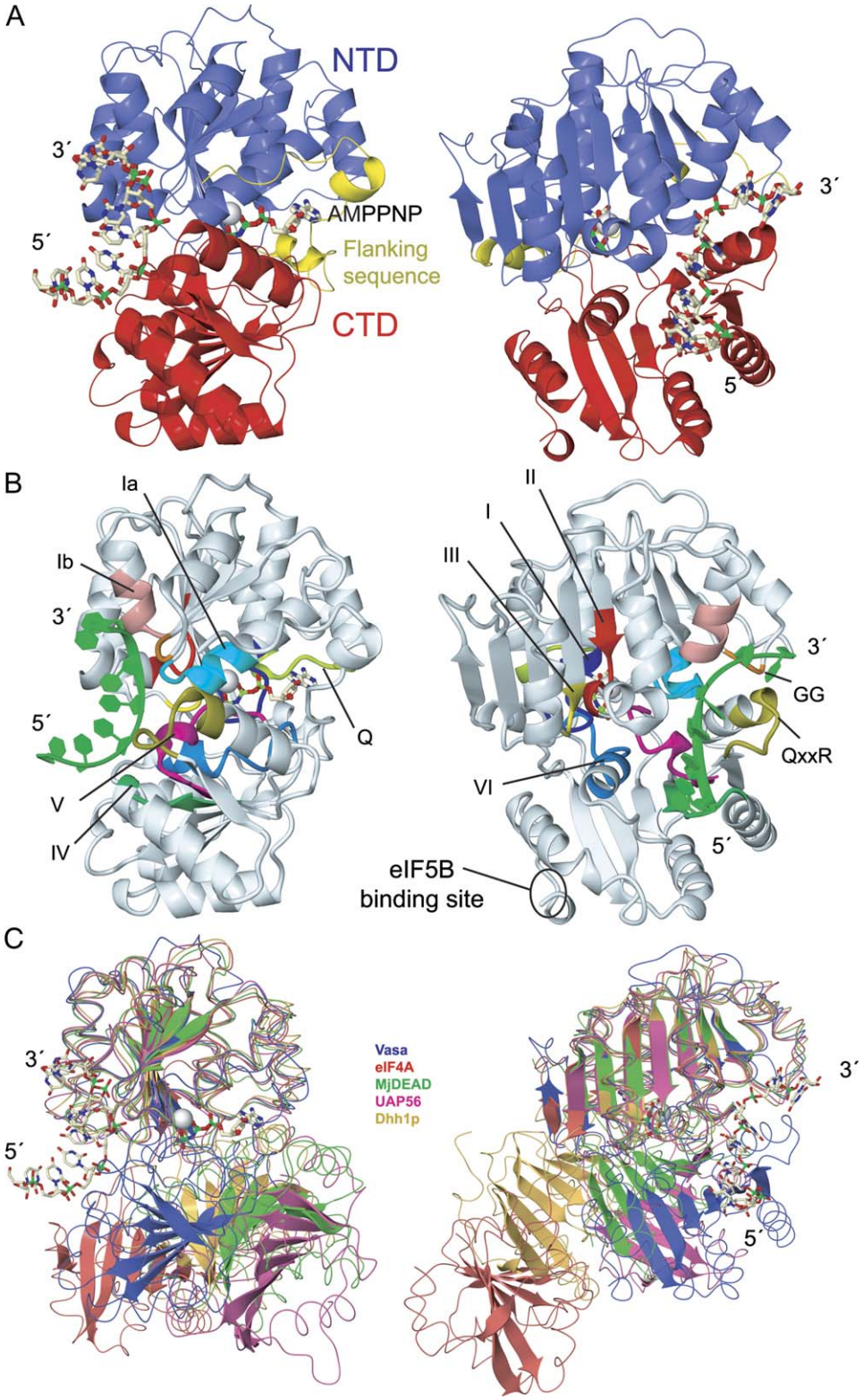

Figure 2. Overall Structure

(A) Front (right) and side (left) views of the Vasa•RNA•AMPPNP complex. The N-terminal domain (NTD), C-terminal domain (CTD), and flanking sequence are colored blue, red, and yellow, respectively. RNA and AMPPNP are shown in a ball-and-stick representation. Mg^{2+} is shown in a space-filling representation.

region, in which the residues are not conserved among the DEAD-box proteins (Figure 1).

The RNA Bound to Vasa Is Bent

The protein-RNA interactions are shown in Figure 3. All of the RNA-interacting residues, except for Arg403 and Glu497, are conserved among the DEAD-box proteins (Figure 1). The NTD and CTD bind the 3′ and 5′ sides of the RNA, respectively (Figure 2 and Figure 3). The phosphate-ribose backbone of the RNA lies along the C-terminal sides of six β strands: The U1–U5 sequence interacts with motif IV (β10), the QxxR motif (β11), and motif V (β12) from the CTD, while the U4–U7 sequence interacts with motif Ia (β3), the GG motif (β4), and motif Ib (β5) from the NTD (Figure 1). U4 and U5 interact with both domains. The protein forms many hydrophilic interactions with the phosphate and 2′-OH groups of the RNA backbone (Figure 3). Four 2′-OH groups are recognized, in agreement with the preference of DEAD-box proteins for RNA over DNA (Rogers et al., 2001). In contrast, the protein does not interact with the base moieties of the RNA, except for one hydrogen bond between the nonconserved Arg403 and U3.

Within the bound RNA, the U1-U2-U3-U4-U5 bases and the U6-U7 bases are individually stacked, but the U5 and U6 bases are not stacked with each other (Figure 3D). Thus, the overall conformation of the RNA is sharply bent between U5 and U6. The rotamers along the U5-U6 backbone, O3′-P-(α)-O5′-(β)-C5′-(γ)-C4′-C3′, are unusual *trans*(α)-*gauche*$^+$(β)-*trans*(γ) forms (Figure 3A and Figure S1). The U6 phosphate, located at the bending point, is extensively recognized by the amide groups of Gly354 (GG) and Arg378 (Ib) and the side chains of Arg328 (Ia) and Thr375 (Ib). The U7 phosphate is recognized by the amide group of Gly355 (GG) and the side chain of Arg378 (Ib), whereas the 2′-OH group of U6 is recognized by the side chains of Arg378 and Asp381 (Ib) (Figures 3A and 3D). When an A form RNA duplex was modeled on the Vasa protein by superposition of one of the two strands on the U1–U5 region of the bound ssRNA, the modeled nucleotide corresponding to U6 sterically clashed with the α7 helix (Figure 3E). The structural comparison of the NTDs revealed that the positions of the α7 helix of Vasa and its equivalents in other DEAD-box proteins are well conserved (Figure 3F). In contrast, the α7 helix equivalents of the SF2 proteins belonging to other subfamilies are not superposable and would cause no steric clash (Figure 3G). Therefore, the bent structure of the bound RNA seems to be a unique feature of the DEAD-box proteins and is likely to be important for their mechanism (see below).

The U1–U5 region interacts with both domains (Figures 3A–3D). The U5 phosphate is bound with the main chain of Arg328 (Ia) and the side chain of Arg528 (QxxR), while its 2′-OH group is bound with the main chain of Gly377 (Ib). The Arg528 equivalents in eIF4A and Dhh1p were predicted to bind RNA (Caruthers et al., 2000; Cheng et al., 2005). The U4 phosphate is bound with the side chain of Thr546 (V) and the main chain of Gly521 (QxxR), while its 2′-OH group is bound with the main chain of Pro326 (Ia). The U3 phosphate is bound with the main chain of Lys499 (IV), while the 2′-OH group of U2 is bound with the side chain of Glu497 (IV).

Furthermore, a network of interdomain interactions is formed at the RNA binding site (Figures 3B and 3D). Two of the RNA binding arginines, Arg328 and Arg528, stack with each other and form interdomain interactions with Gln525 (QxxR) and Glu329 (Ia), respectively. In addition, Gln525 and Glu329, which are well conserved among the DEAD-box proteins, interact with each other. Therefore, the conserved hydrophilic residues of the two domains form complicated interactions, thus creating the continuous RNA binding surface. Probably because of the interdomain interactions, the conformation of the QxxR motif is characteristically different from those of other DEAD-box proteins without bound RNA (Figure S2). These features are characteristic of the closed form.

ATP Binding and Hydrolysis Mechanisms

The ATP binding pocket is formed between the two RecA-like domains. AMPPNP interacts with the amino acid residues from the flanking sequence, the Q motif, motif I (also known as the Walker A motif or P loop), motif II (the Walker B motif), motif V, and motif VI (Figure 1 and Figure 3). Motif V is the only motif that interacts with both the RNA and AMPPNP. Except for the residues in the Vasa-specific flanking sequence, all of the residues involved in the ATP binding and hydrolysis are conserved among the DEAD-box proteins (Figure 1). The conformations of motifs III, V, and VI significantly differ from those of other ATP-free DEAD-box proteins (Figure S2).

From the flanking sequence, Phe225 makes a van der Waals interaction with the adenine base (Figure S3). From the NTD, motifs I and II and the Q motif interact with the AMPPNP (Figure 3A and Figure S3) in a manner similar to in the structures of eIF4A and UAP56 (Benz et al., 1999; Shi et al., 2004). Moreover, the higher resolution enabled us to precisely locate the bound water molecules around AMPPNP and Mg^{2+}. The Q motif recognizes the adenine moiety of AMPPNP, while motifs I and II bind the triphosphate moiety, directly and through a Mg^{2+} ion and water molecules. From the CTD, motifs V and VI directly interact with the ribose and the triphosphate moieties of AMPPNP, respectively (Figures 4A and 4B): The carboxyl group of Asp554 (V) hydrogen bonds with the 3′-OH group (Figure 4A and Figure S3); Arg582 (VI) binds all of the α-, β-, and γ-phosphates; and Arg579 (VI) interacts with the γ-phosphate (Figure 4B).

(B) Locations of the conserved motifs. The bound RNA is colored green.
(C) Superimposition of the NTDs of Vasa, eIF4A, MjDEAD, and UAP56. The β sheets are shown in a ribbon representation. Same view as in (A) and (B).

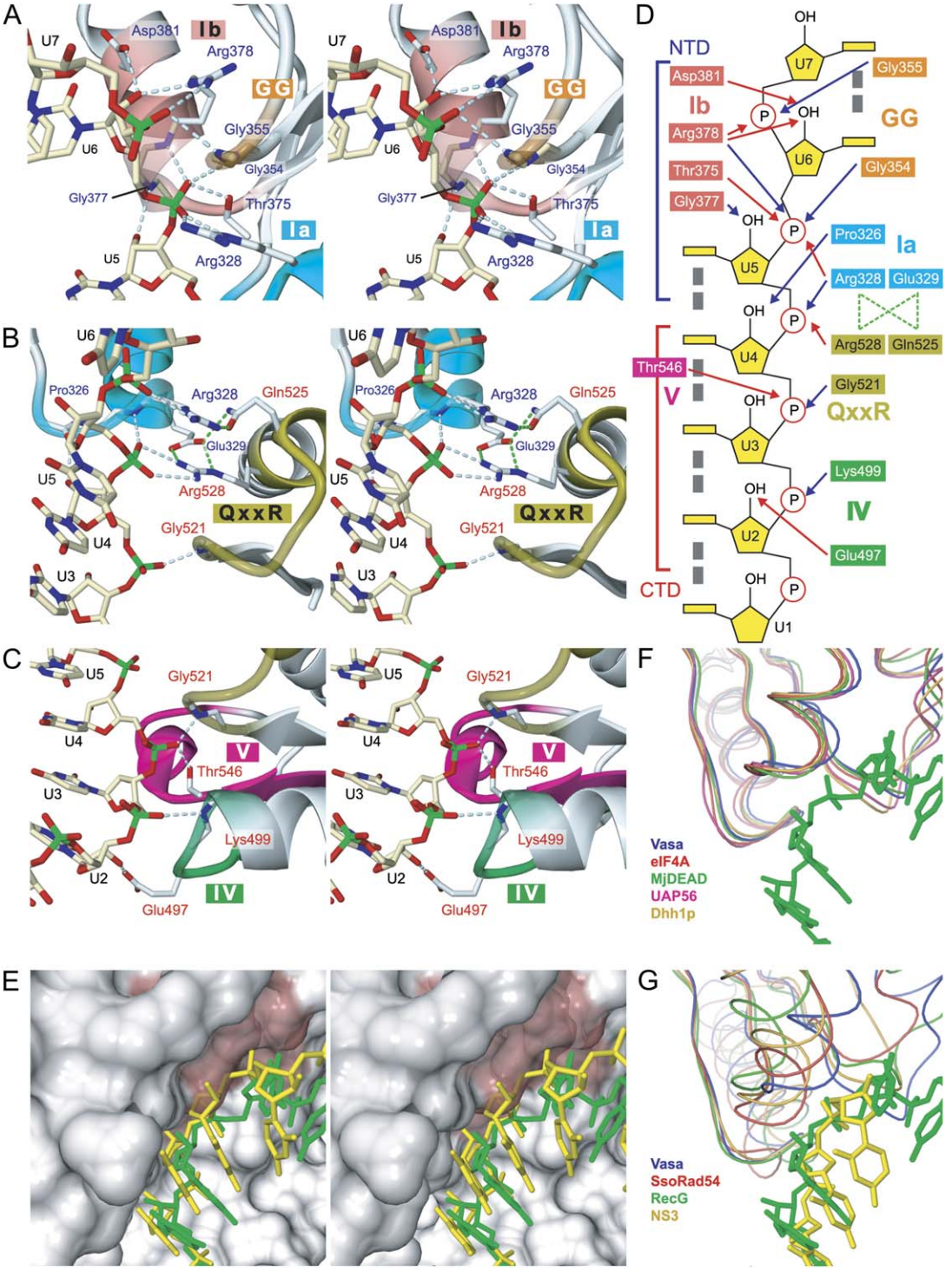

Figure 3. RNA Binding and Bending

Blue and red characters indicate residues from the NTD and CTD, respectively. Green broken lines indicate interdomain interactions.

(A) Stereo view near the bending point.

(B) Stereo view of the U4-U5 region.

(C) Stereo view of the U2-U3 region.

(D) Schematic representation. Blue and red arrows indicate interactions through the main chains and the side chains of amino acid residues, respectively. Gray boxes indicate base stacking.

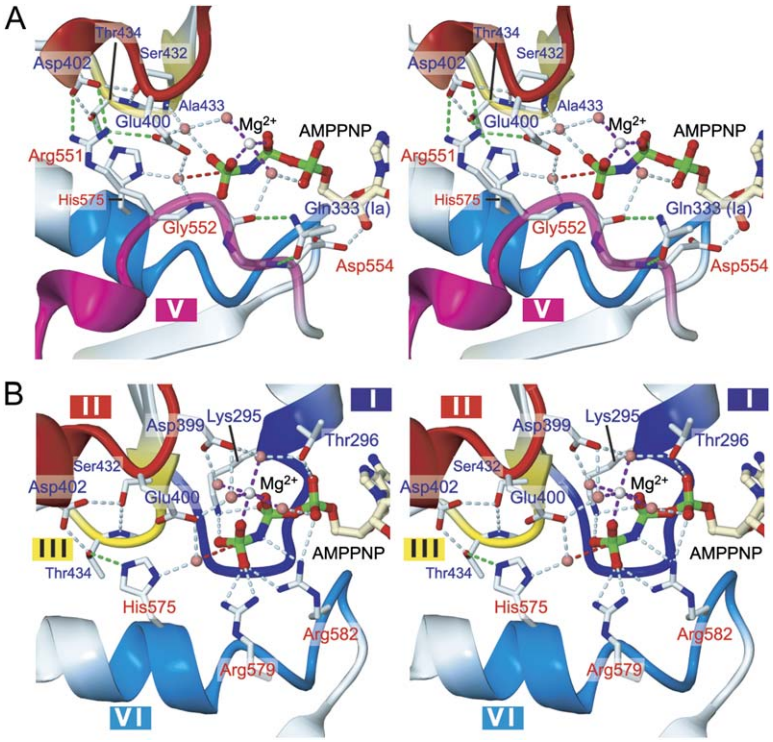

Figure 4. ATPase Site Stereo Views

Blue and red characters indicate residues from the NTD and CTD, respectively. Water molecules are shown as pink spheres. Purple and green broken lines indicate coordinated bonds and interdomain interactions, respectively. The red broken line connects the presumptive attacking water and the γ-phosphorus atom.

(A) Triphosphate binding. Motif V is omitted for clarity.

(B) Motif V is involved in AMPPNP binding, attacking water binding, and interdomain interactions. Motif I and the backbone of motif Ia, to which Gln333 belongs, are omitted for clarity.

We identified one water molecule as the presumptive attacking water for ATP hydrolysis (Figures 4A and 4B). This water is well ordered (B factors of 16–22 $Å^2$ for the four complexes in the asymmetric unit), 3.25 Å away from the γ-phosphorus atom, and located ideally for a nucleophilic in-line attack. The side chains of Glu400 (II) and His575 (VI) and the main-chain amide group of Gly552 (V) interact with this water. In eIF4A, mutations of the equivalents of Glu400 and His575 significantly reduced the ATPase activity and abolished the unwinding activity (Pause et al., 1993; Pause and Sonenberg, 1992). Mutations of the equivalents of Arg579 and Arg582 also decreased the ATPase activity of eIF4A (Pause et al., 1993). These arginines may contribute to the ATPase reaction in a manner similar to that of the "arginine finger" of the GTPase-activating protein for Ras (Scheffzek et al., 1997).

Motif III is the only motif that does not interact with either RNA or AMPPNP in the present structure. Instead, it interacts with motifs II and VI: Ser432 (III) and Thr434 (III) make intradomain interactions with Asp402 (II), and Thr434 makes an interdomain interaction with His575 (VI). Furthermore, motif V joins this interaction network: The His575 side chain stacks with the Arg551 side chain from motif V, and Arg551 forms interdomain interactions with Glu400 and Asp402. Gln333 (Ia) also makes interdomain interactions with Gly552 and Asp554. Therefore, motifs Ia, II, III, V, and VI form a complicated interaction network near the ATPase site (Figure 4A).

The simultaneous replacement of Ser213 and Thr215 of eIF4A (motif III, corresponding to Ser432 and Thr434 of Vasa, respectively) with alanine (the AAA mutant) abolished the unwinding activity without reducing the RNA binding and ATPase activities (Pause and Sonenberg, 1992). Similarly, the histidine substitution for Asp185 of eIF4A (motif II, corresponding to Asp402 of Vasa) (the DEAH mutant) impaired only the overall unwinding activity (Pause and Sonenberg, 1992). The product of the vas^{D5} allele has the G552D mutation in motif V, and the recombinant mutant protein is active in both RNA binding and ATP hydrolysis but defective in unwinding (Liang et al., 1994). Therefore, these conserved residues, which are involved in the interdomain interactions, are important for unwinding.

Mutations that Affect Interdomain Interactions Uncouple ATP Hydrolysis and RNA Unwinding

The present Vasa structure reveals that all of the 11 conserved motifs participate in the ATP binding, RNA binding, and/or interdomain interactions (Figure 1, Figure 3, and Figure 4). To examine the roles of these conserved residues in the unwinding mechanism, we carried out mutant

(E) Surface representation of the protein near the α7 helix (stereo view). Motif Ib is colored pink. The bound RNA and the modeled straight RNA are colored green and yellow, respectively.

(F) The α7 helix and its equivalents in DEAD-box proteins. The RNA bound to Vasa is colored green.

(G) The α7 helix and its equivalents in various SF2 proteins. The bent RNA bound to Vasa and the straight DNA bound to NS3 are colored green and yellow, respectively.

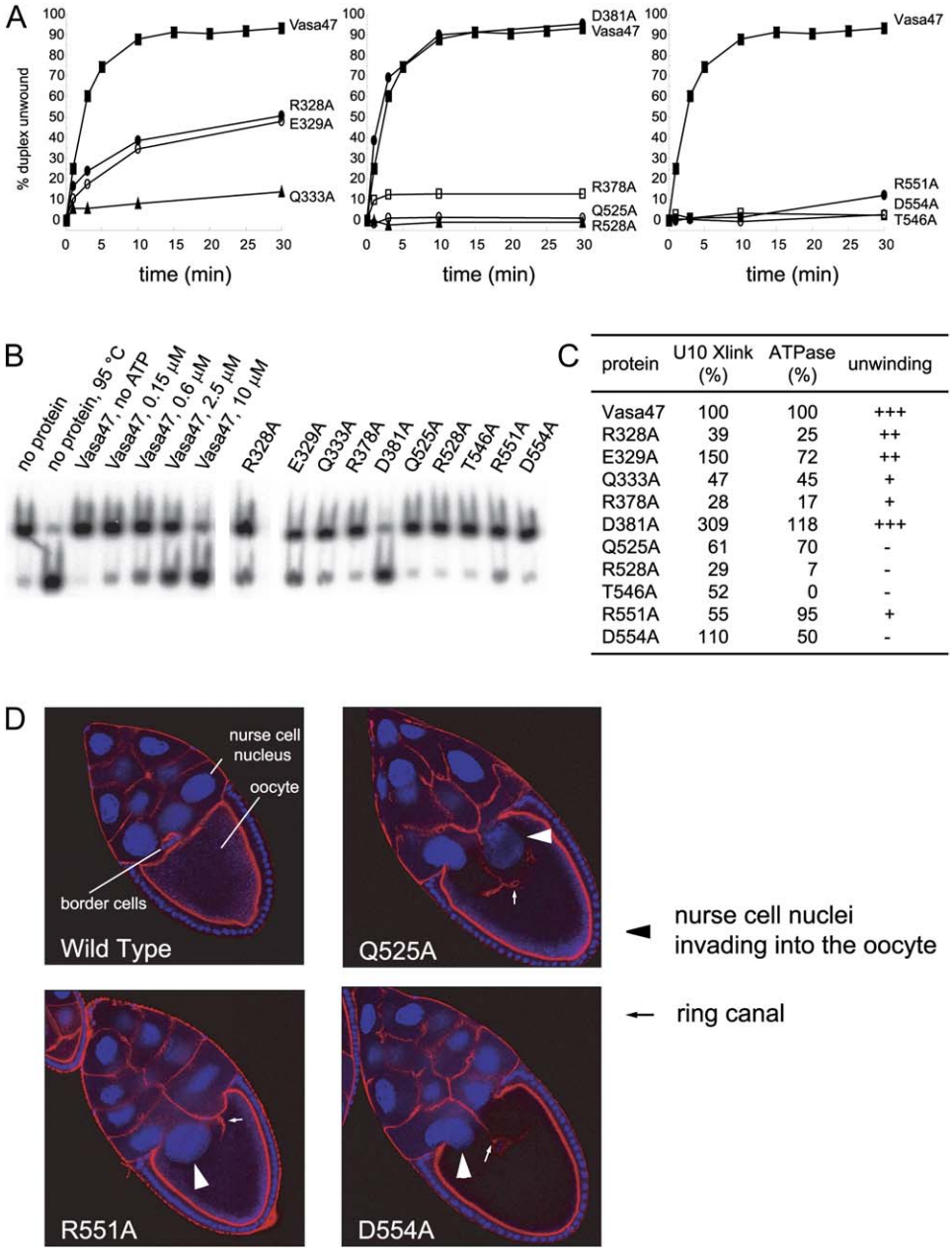

protein	U10 Xlink (%)	ATPase (%)	unwinding
Vasa47	100	100	+++
R328A	39	25	++
E329A	150	72	++
Q333A	47	45	+
R378A	28	17	+
D381A	309	118	+++
Q525A	61	70	-
R528A	29	7	-
T546A	52	0	-
R551A	55	95	+
D554A	110	50	-

Figure 5. Mutational Analyses

(A) Time course of the RNA unwinding by the wild-type or Vasa47 mutants.

(B) RNA unwinding after a 30 min incubation.

(C) Summary of the biochemical activities. U10-RNA crosslinking and RNA-stimulated ATPase activities are shown as percentages of the wild-type Vas47 activity. Unwinding activity: +++, similar to that of the wild-type Vas47; ++, moderately reduced; +, strongly reduced; −, not detected.

(D) Egg chambers of flies expressing wild-type or mutant Vasa. Blue, DAPI; red, F-actin (phalloidin).

analyses. First, Vasa47, which is the Vasa helicase fragment used in the structure determination, was tested for its UV-induced RNA-crosslinking, ATPase, and unwinding activities. Vasa47 crosslinked to U10 RNA in an AMPPNP-dependent manner (Figure S4), in agreement with our previous result with a longer protein fragment (Sengoku et al., 2004). Vasa47 exhibited ATPase activity (Figure S4), which was, like eIF4A, dependent on RNA (data not shown). Finally, like eIF4A (Rogers et al., 2001), Vasa47 unwound a blunt-ended 13-mer RNA duplex in an ATP-dependent manner (Figure 5B). These results confirm that Vasa47 has the conventional DEAD-box helicase activity even though it is truncated by about 200 and 40 residues at its N and C termini, respectively. We then

produced mutant Vasa47 proteins with an alanine substitution for Arg328, Glu329, Gln333, Arg378, Asp381, Gln525, Arg528, Thr546, Arg551, or Asp554. All of these residues are widely conserved within the DEAD-box family and either interact with the RNA (Arg328, Arg378, Asp381, Arg528, and Thr546) or AMPPNP (Asp554) or participate in the interdomain interactions (Glu329, Gln333, Gln525, Arg551, and Asp554) (Figure 1).

The biochemical activities of the mutants are shown in Figures 5A and 5B and Figure S4 and are summarized in Figure 5C. The RNA-crosslinking activity was remarkably reduced by the R328A, R378A, and R528A mutations. Furthermore, the RNA-dependent ATPase and unwinding activities of these mutants were also affected. The R528A mutant exhibited barely detectable ATPase activity and was completely defective in unwinding. The ATPase and unwinding activities of the R378A mutant were both significantly reduced, while those of the R328A mutant were less affected. Similarly, the T546A mutation abolished both the ATPase and unwinding activities, while it moderately decreased the RNA crosslinking. Note that Arg328, Arg378, Arg528, and Thr546 are the four residues, among those tested, that interact with the RNA phosphates in the crystal structure (Figure 3). Consequently, the interaction with the RNA phosphates is important for both the ATPase and unwinding activities. In contrast, the replacement of Asp381, whose side chain interacts with only the 2′-OH group of U6, did not reduce the activities; the RNA crosslinking of the D381A mutant was actually enhanced (Figure 5C). This increased crosslinking may be caused by the elimination of the electrostatic repulsion between the Asp381 side chain and the RNA phosphates.

The RNA-crosslinking activity was also increased by the mutation of Glu329, near the RNA binding site, but was not affected much by that of Asp554, in the ATP binding site. The other mutations, Q333A, Q525A, and R551A, moderately decreased the RNA-crosslinking activity. These five mutations only moderately or negligibly affected the ATPase activity. Nevertheless, the unwinding activity was abolished by the Q525A and D554A mutations and was drastically reduced by the Q333A and R551A mutations. The E329A mutation decreased the unwinding activity as much as the R328A mutation, whereas the E329A mutant was significantly more active in ATP hydrolysis (Figure 5C). Thus, the ATPase and unwinding activities are uncoupled in the E329A, Q333A, Q525A, R551A, and D554A mutants.

Glu329, Gln333, Gln525, and Arg551 are not involved in the binding of RNA or AMPPNP, but, instead, they participate in the interdomain interactions (Figure 3 and Figure 4). Asp554 also makes an interdomain interaction with Gln333, in addition to the interaction with the AMPPNP 3′-OH group (Figure 4A). As noted above, in the AAA and DEAH mutants of eIF4A and the product of the *vas*^{D5} allele, the mutations of the residues involved in the interdomain interactions uncoupled the ATPase and unwinding activities (Liang et al., 1994; Pause and Sonenberg, 1992). Taken together, these results highlight a common feature of the uncoupling mutations: They are all involved in the interdomain interactions.

We further investigated the in vivo effects of the uncoupling mutations. The Q525A, R551A, and D554A mutations were each introduced into the full-length Vasa protein. When the mutant proteins were expressed during *Drosophila* oogenesis under the control of the *nanos*-Gal4VP16 driver, they caused oogenesis defects in about 5% of the egg chambers. We found that the defective egg chamber lost its integrity at the boundary between the nurse cells and the oocyte, and the nurse-cell nuclei invaded the region that the oocyte normally occupies (Figure 5D). These defects were never observed when the wild-type Vasa was expressed by the same methods (Figure 5D). Intriguingly, similar oogenesis defects have been observed in ovaries null for *vasa* (Styhler et al., 1998; Tomancak et al., 1998). Consequently, the uncoupled mutants of Vasa seem to be capable of acting in a dominant-negative manner. Similarly, when Gly346 of Dhh1p was replaced by alanine, the mutant protein exhibited a dominant-negative phenotype in yeast (Cheng et al., 2005). Actually, the corresponding residue in Vasa, Gly552, forms an interdomain interaction with Gln333 (Figure 4B).

DISCUSSION

ATP-Dependent RNA Binding and RNA-Dependent ATP Hydrolysis

The DEAD-box proteins interact with RNA and ATP in a mutually related manner. First, the binding of ATP increases the affinity for RNA, and vice versa. Second, the hydrolysis of the bound ATP strictly requires the RNA binding (Lorsch and Herschlag, 1998; Polach and Uhlenbeck, 2002; Sengoku et al., 2004). The closed-form Vasa structure determined in this study provides the basis for the interdependent interactions with ATP and RNA, as follows. In the closed form, the bound ATP interacts extensively with the pocket created by the two domains (Figure 4), and, separately, the RNA spans the two domains and makes many interactions (Figure 3). ATP and RNA bind to the closed form much more strongly than to the open forms and thus stabilize the closed form, which underlies their cooperative binding. Consequently, the functional ATPase site with the attacking water molecule is organized in the closed form, as observed here, which results in ATP hydrolysis. After the ATP hydrolysis, the closed form is no longer stabilized, and the affinity for RNA should be reduced.

In accordance with these structural features, the mutations of the ATP binding residues impaired the RNA binding activity, and those of the RNA binding residues eliminated the ATPase activity. When one of the two arginine residues that interact with ATP in eIF4A (Arg362 and Arg365, corresponding to Vasa Arg579 and Arg582, respectively) was replaced by glutamine or lysine, the RNA crosslinking to the mutant proteins was drastically reduced (Pause et al., 1993). As described above, the Vasa47 R528A and T546A mutations, which replace an

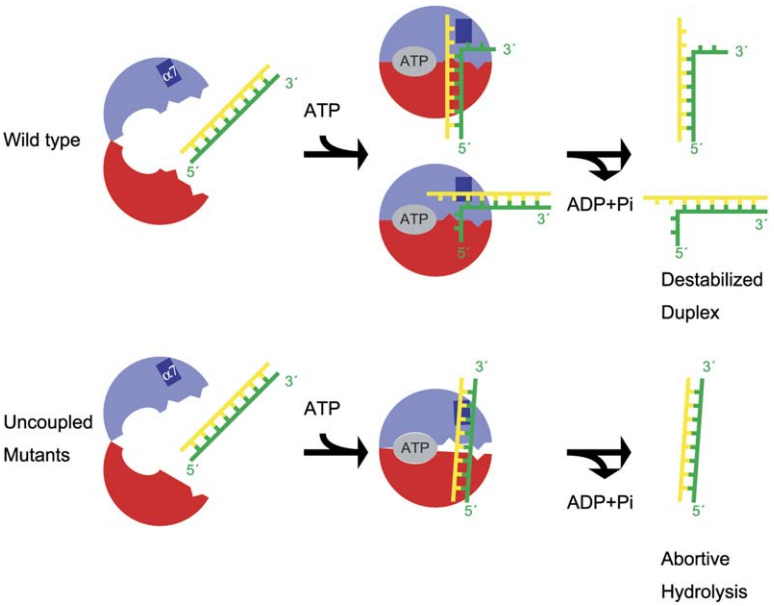

Figure 6. Proposed Mechanisms of RNA Unwinding by the DEAD-Box Protein and Abortive ATP Hydrolysis by the Uncoupled Mutants

RNA binding residue in the CTD with alanine, almost completely abolished the RNA-dependent ATPase activity.

RNA Bending Disrupts Neighboring Base Pairs

A striking feature in the present structure is the sharp bend between U5 and U6 of the bound RNA near the α7 helix in the NTD (Figure 2 and Figure 3). The RNA bending is clearly incompatible with continuous base pairing. Short, blunt-ended, double-stranded RNA (dsRNA) is unwound by Vasa, as well as by eIF4A (Rogers et al., 2001). If the DEAD-box protein induces the bend by binding to one of the two strands of the dsRNA, then the base pairs on either the 3′ or 5′ side of the bend must be disrupted (Figure 6). Such bending may be facilitated by thermal fraying of the terminal base pair of the duplex. The loss of the base-pairing interactions may be compensated by the large number of newly formed interactions between the protein and the bound strand. Therefore, the bend may cause partial melting and destabilization of the dsRNA, which is fundamental to unwinding the RNA duplex. In fact, we could successfully model the structures of the complex between Vasa and a destabilized dsRNA by placing an oligo-A strand complementary to the U1–U5 or U6-U7 region of the bound strand in the crystal structure (Figure S5). In the model, there is no conserved amino acid residue near the complementary RNA strand, suggesting that the complementary strand does not interact specifically with the protein. In agreement with the present model, biochemical analyses indicated that eIF4A mainly interacts with only one strand of the duplex, and any interaction with the complementary strand is minimal (Rogers et al., 2001).

Release of the Unwound RNA upon ATP Hydrolysis

We propose a plausible mechanism of RNA unwinding. The two RecA-like domains, which have a quite dynamic arrangement in the free form, cooperatively bind ATP and one strand of the duplex region. Upon binding, the protein induces bending of the bound RNA strand, thereby separating the base pairs on either the 5′ or 3′ side of the bend. Which base pairs are disrupted may depend on their relative stability. If the substrate RNA has a single-stranded tail on the 5′ side of the duplex region, then the protein could catch the tail and accommodate it at the positions corresponding to U1–U3 in the crystal structure, thereby unwinding the duplex more efficiently. In agreement with this, a short single-stranded tail attached on the 5′ side of the duplex facilitates RNA unwinding by eIF4A more effectively than that on the 3′ side (Rogers et al., 2001). After RNA binding and bending, the protein hydrolyzes ATP and may subsequently release the partially disrupted duplex. Therefore, nonhydrolyzable ATP analogs should inhibit the turnover of the helicase. Once it is partially disrupted, the duplex would be unstable and more susceptible to complete separation of the strands. The protein-RNA dissociation activity of Ded1p (Fairman et al., 2004) may also be explained by RNA bending.

Interdomain Interactions Ensure that the RNA Is Bent Prior to ATP Hydrolysis

The bent region of the RNA strand is located near the α7 helix, and they interact extensively. If the A form conformation of the U1–U5 region of the bound RNA strand extended straight up to U6, then the ribose moiety of U6 would clash sterically with the α7 helix (Figure 3E). Thus, the location of the α7 helix would inevitably induce the bending of the bound RNA strand, and the steric clash would be avoided if the RNA shifted by about 3 Å away from the α7 helix (Figure 3E). Therefore, the accurate positioning of the RNA strand relative to the α7 helix is necessary for bending. As the RNA spans the two domains,

its position relative to the α7 helix would be influenced by the arrangement of the two domains. Furthermore, the binding of the RNA strand near the bend is maintained by a number of interactions involving residues from both domains. For example, the side chains of Arg328 (NTD) and Arg528 (CTD) interact with the U6 and U5 phosphates, respectively, and are fixed at their positions by the interdomain interactions with Gln525 (CTD) and Glu329 (NTD), respectively, as well as with each other (Figure 3). Consequently, the extensive interdomain interactions may be required to ensure the accurate positioning and bending of the RNA strand.

The uncoupling mutations would affect the arrangement of the NTD and CTD and/or the accurate positioning of the RNA near the α7 helix. As a result, the mutant protein would still be able to bind RNA but would not be able to induce the bending of the bound RNA. On the other hand, the geometry of the ATPase site would not be seriously affected, as the RNA binding and ATPase sites are distal and proximal to the linker region, respectively. Therefore, the mutant proteins are able to bind RNA and to hydrolyze ATP but are unable to induce the bending of the bound RNA, resulting in abortive ATP hydrolysis (Figure 6). In other words, the interdomain interactions are essential for coupling ATP hydrolysis to RNA bending.

The DEAD-Box Helicase Core Is a Compact Unit for Regulated RNA Unwinding, in Contrast to those of Translocating RNA Helicases

In this unwinding mechanism, the helicase core, consisting of the two RecA-like domains, can act as an ATP-driven helix-destabilizing unit. Most DEAD-box proteins possess auxiliary domains other than the core, and many DEAD-box proteins are thought to act in concert with other protein cofactors (Silverman et al., 2003). The additional domain and/or factor may interact with the RNA substrate in a site-specific or nonspecific manner, thereby conferring the specificity or increasing the affinity of the DEAD-box protein. Consequently, the in vitro and in vivo functions of each DEAD-box protein depend on the additional domain/factor (or factors), although the highly conserved helicase core is likely to function in fundamentally the same manner. For example, the unique C-terminal domain of DbpA anchors to hairpin 92 of the 23S ribosomal RNA, determining the specificity for the duplex to be unwound (Fuller-Pace et al., 1993; Nicol and Fuller-Pace, 1995). The 3′→5′ directionality and the requirement of the single-stranded spacer of DbpA (Diges and Uhlenbeck, 2005) may be a consequence of the position of the helicase core relative to the unique domain.

The proposed mechanism is drastically different from those for other helicases or motors acting on nucleic acids. The canonical helicases are considered to processively unwind the double-stranded region of the nucleic acid by first binding to the single-stranded loading strand and then translocating on the strand with multiple rounds of ATP hydrolysis. For example, a vaccinia virus DExH-box protein, NPH-II, unwinds 3′-tailed long dsRNAs with strong processivity (Jankowsky et al., 2000). Some of the SF2 helicases combine the tandem RecA-like domains, which act as a translocation motor, with an additional domain that acts as a wedge to destabilize the duplex (Singleton and Wigley, 2002). In contrast, some DEAD-box proteins are able to unwind blunt-ended dsRNAs. Furthermore, the tandem RecA-like domains of the DEAD-box proteins by themselves can act as the helix-destabilizing unit, without the need for auxiliary wedge domains. For that purpose, the DEAD-box proteins contain an internal "wedge helix" in the NTD (the α7 helix in Vasa) to bend the bound RNA strand. However, the bend in the RNA may make it difficult for the DEAD-box proteins to translocate on one strand of the RNA for processive unwinding.

These mechanistic differences seem to be correlated with the cellular functions of the DEAD-box proteins. Cellular RNAs exhibit a variety of higher-order structures, in which a long continuous stretch of dsRNA is rarely formed. Presumably, the target sites of the DEAD-box proteins would often be a short duplex within a higher-order RNA structure. For example, *Neurospora crassa* CYT-19 specifically disrupts four base pairs delimited by short internal loops, in the middle of a long hairpin in the group I intron misfolded intermediate, probably without affecting other base pairs (Mohr et al., 2002). Other examples of the target sites are base pairs formed intramolecularly or intermolecularly in ribonucleoprotein complexes, such as spliceosomes and ribosome assembly intermediates. These target dsRNAs exist in a naturally crowded environment with other parts of RNAs and attached proteins. These jobs are not suitable for the canonical translocating helicases. The processivity of the canonical translocating helicases may even be deleterious in these systems, as they could disrupt the functional RNA structures. In contrast, the DEAD-box protein minimal core, with the internal wedge helix, can directly bind to the target site and can locally modulate the targeted RNA structure. Furthermore, the DEAD-box proteins may minimize the undesirable disruption of the surrounding base pairs since they do not require translocation on the RNA. These unique features may enable the DEAD-box proteins to be involved in specific, yet ubiquitous, roles in RNA metabolism and regulation.

Common Features among SF2 Proteins

The SF2 proteins share the two-RecA-like-domain architecture (Caruthers and McKay, 2002), as well as most of the residues involved in ATP binding. Moreover, the two RNA binding threonine residues of motifs Ib and V are also conserved or conservatively substituted with serine in the SF2 proteins. On the other hand, most of the residues involved in RNA bending or interdomain interactions are strictly conserved among the DEAD-box proteins but not in other SF2 proteins. Although the unwinding mechanism of the DEAD-box proteins is different from those of other SF2 proteins, the collaboration of the two domains for substrate binding and ATP hydrolysis seems to be

common in most of the SF2 proteins. The present Vasa structure, which is the first ATP bound, closed form of an SF2 protein, should provide a basis for modeling the functional ATP bound forms of other SF2 proteins.

EXPERIMENTAL PROCEDURES

Crystallization and Data Collection

The Vasa helicase region (residues 200–623) in complex with RNA and AMPPNP was crystallized as described (Sengoku et al., 2004). The native crystals belong to the space group $P2_1$ (a = 71.06 Å, b = 142.35 Å, c = 130.47 Å, β = 90.86°). The SeMet-substituted crystals were obtained similarly, but HEPES buffer (pH 7.4) and polyethylene glycol (PEG) 20000 were used instead of ADA buffer (pH 6.5) and PEG 4000, respectively. Crystals were flash frozen in a nitrogen stream at 100 K. All data sets were collected on BL41XU at SPring-8.

Structure Determination

The diffraction data were processed and scaled with DENZO and SCALEPACK (Otwinowski and Minor, 1997). The selenium sites were located by SnB (Weeks and Miller, 1999). Initial phases were calculated by SHARP (de La Fortelle and Bricogne, 1997), and the density modification was carried out by DM (CCP4, 1994). The model was automatically constructed and refined by RESOLVE (Terwilliger and Berendzen, 1999) and refmac (CCP4, 1994) followed by manual modification using O (Jones et al., 1991) and refinement by CNS (Brunger et al., 1998). Figure 1 was prepared using CLUSTAL W (Thompson et al., 1994) and ESPript (Gouet et al., 1999). Structural figures were prepared using Que and Cuemol (http://cuemol.sourceforge.jp/en/).

RNA Crosslinking and ATPase Assays

The RNA crosslinking assay was carried out as described (Sengoku et al., 2004). The ATPase activity was monitored by a coupled pyruvate kinase-lactate dehydrogenase assay (Bessman, 1963) at 24°C. Reactions were performed in 20 mM MES-Na buffer (pH 6.0) containing 50 mM potassium acetate, 2.5 mM $MgCl_2$, 2.5 mM ATP, 1 mM DTT, 10% glycerol, 2 mM phospho(enol)pyruvate, 0.3 mM NADH, 3 units/ml lactate dehydrogenase (Sigma), 3 units/ml pyruvate kinase (Sigma), 130 μg/ml yeast total RNA (Sigma), and 100 μg/ml Vasa47. The oxidation of NADH to NAD^+ was monitored at 338 nm.

Unwinding Assay

Equimolar amounts of ^{32}P-labeled R13 (GCUUUACGGUGCU) and unlabeled R13C (AGCACCGUAAAGC) (Rogers et al., 2001) were mixed in 10 mM Tris-HCl buffer (pH 8.0) containing 50 mM KCl, 1 mM EDTA, and 40 units/ml RNase inhibitor and were heated at 95°C for 5 min, followed by slow cooling to 4°C over 90 min. Then, the annealed duplex was purified by native PAGE. Unwinding of the duplex was monitored by following the displacement of the labeled strand from the duplex at 24°C. The reaction mixture was 20 mM Tris-HCl buffer (pH 8.0) containing 65 mM NaCl, 50 mM KCl, 1 mM DTT, 2 mM $MgCl_2$, 2 mM ATP, 10% glycerol, 400 units/ml RNase inhibitor, 10 μM Vasa47, 25 nM duplex, and 500 nM unlabeled R13 ("trap" RNA) (Bizebard et al., 2004). At the indicated times, aliquots (10 μl) were mixed with 7 μl of 140 mM Tri-HCl buffer (pH 8.0) containing 70 mM EDTA, 1.4% SDS, 0.02% bromophenol blue, 0.02% xylene cyanol, 28% glycerol, and 0.6 mg/ml Proteinase K and were incubated for 2 min at 24°C. The mixtures were subjected to native PAGE on a 20% polyacrylamide gel.

In Vivo Assay of *vasa* Mutants

To express the wild-type and mutant Vasa proteins in the germline cells, males possessing UASp-*vasa* transgenes (Rorth, 1998) were crossed with *nanos*-Gal4VP16 females. Ovaries from females possessing both the UASp-*vasa* and *nanos*-Gal4VP16 transgenes were dissected in PBS, fixed for 30 min in 4% paraformaldehyde in PBS, and incubated for 1 hr in PBS-0.2% Tween 20 containing DAPI (1 μg/ml) and Alexa 594-conjugated phalloidin (4 U/ml; Invitrogen). After the ovaries were washed with PBTw, they were mounted in Vectashield (Vector Labs). The ovaries were observed under a laser scanning confocal microscope (Leica TCS-SP2 AOBS).

Supplemental Data

Supplemental Data include five figures and can be found with this article online at http://www.cell.com/cgi/content/full/125/2/287/DC1/.

ACKNOWLEDGMENTS

We thank M. Kawamoto and H. Sakai (JASRI) for their help in data collection at SPring-8 and S. Fukai, R. Ishitani, and R. Ishii for their advice on protein purification, crystallization, and crystallographic analysis. This work was supported by a Grant-in-Aid for Scientific Research S from the Japan Society for the Promotion of Science (JSPS); Grants-in-Aid for Scientific Research in Priority Areas from the Ministry of Education, Culture, Sports, Science and Technology (MEXT) of Japan; and the RIKEN Structural Genomics/Proteomics Initiative (RSGI) in the National Project on Protein Structural and Functional Analyses, MEXT.

Received: October 18, 2005
Revised: December 15, 2005
Accepted: January 27, 2006
Published: April 20, 2006

REFERENCES

Benz, J., Trachsel, H., and Baumann, U. (1999). Crystal structure of the ATPase domain of translation initiation factor 4A from Saccharomyces cerevisiae—the prototype of the DEAD box protein family. Structure *7*, 671–679.

Bessman, M.J. (1963). Deoxynucleoside monophosphate kinases. Methods Enzymol. *6*, 166–176.

Bizebard, T., Ferlenghi, I., Iost, I., and Dreyfus, M. (2004). Studies on three E. coli DEAD-box helicases point to an unwinding mechanism different from that of model DNA helicases. Biochemistry *43*, 7857–7866.

Breitwieser, W., Markussen, F.H., Horstmann, H., and Ephrussi, A. (1996). Oskar protein interaction with Vasa represents an essential step in polar granule assembly. Genes Dev. *10*, 2179–2188.

Brunger, A.T., Adams, P.D., Clore, G.M., DeLano, W.L., Gros, P., Grosse-Kunstleve, R.W., Jiang, J.S., Kuszewski, J., Nilges, M., Pannu, N.S., et al. (1998). Crystallography & NMR system: A new software suite for macromolecular structure determination. Acta Crystallogr. D Biol. Crystallogr. *54*, 905–921.

Carmel, A.B., and Matthews, B.W. (2004). Crystal structure of the BstDEAD N-terminal domain: A novel DEAD protein from Bacillus stearothermophilus. RNA *10*, 66–74.

Carrera, P., Johnstone, O., Nakamura, A., Casanova, J., Jackle, H., and Lasko, P. (2000). VASA mediates translation through interaction with a Drosophila yIF2 homolog. Mol. Cell *5*, 181–187.

Caruthers, J.M., and McKay, D.B. (2002). Helicase structure and mechanism. Curr. Opin. Struct. Biol. *12*, 123–133.

Caruthers, J.M., Johnson, E.R., and McKay, D.B. (2000). Crystal structure of yeast initiation factor 4A, a DEAD-box RNA helicase. Proc. Natl. Acad. Sci. USA *97*, 13080–13085.

CCP4 (1994). The CCP4 suite: programs for protein crystallography. Acta Crystallogr. D Biol. Crystallogr. *50*, 760–763.

Cheng, Z., Coller, J., Parker, R., and Song, H. (2005). Crystal structure and functional analysis of DEAD-box protein Dhh1p. RNA *11*, 1258–1270.

Cordin, O., Tanner, N.K., Doere, M., Linder, P., and Banroques, J. (2004). The newly discovered Q motif of DEAD-box RNA helicases regulates RNA-binding and helicase activity. EMBO J. *23*, 2478–2487.

de la Cruz, J., Kressler, D., and Linder, P. (1999). Unwinding RNA in Saccharomyces cerevisiae: DEAD-box proteins and related families. Trends Biochem. Sci. *24*, 192–198.

de La Fortelle, E., and Bricogne, G. (1997). Maximum-likelihood heavy-atom parameter refinement for multiple isomorphous replacement and multiwavelength anomalous diffraction methods. Methods Enzymol. *276*, 472–494.

Diges, C.M., and Uhlenbeck, O.C. (2005). Escherichia coli DbpA is a 3′ → 5′ RNA helicase. Biochemistry *44*, 7903–7911.

Fairman, M.E., Maroney, P.A., Wang, W., Bowers, H.A., Gollnick, P., Nilsen, T.W., and Jankowsky, E. (2004). Protein displacement by DExH/D "RNA helicases" without duplex unwinding. Science *304*, 730–734.

Fuller-Pace, F.V., Nicol, S.M., Reid, A.D., and Lane, D.P. (1993). DbpA: a DEAD box protein specifically activated by 23s rRNA. EMBO J. *12*, 3619–3626.

Gingras, A.C., Raught, B., and Sonenberg, N. (1999). eIF4 initiation factors: effectors of mRNA recruitment to ribosomes and regulators of translation. Annu. Rev. Biochem. *68*, 913–963.

Gorbalenya, A.E., and Koonin, E.V. (1993). Helicases: amino acid sequence comparisons and structure-function relationships. Curr. Opin. Struct. Biol. *3*, 419–429.

Gouet, P., Courcelle, E., Stuart, D.I., and Metoz, F. (1999). ESPript: analysis of multiple sequence alignments in PostScript. Bioinformatics *15*, 305–308.

Hay, B., Jan, L.Y., and Jan, Y.N. (1988). A protein component of Drosophila polar granules is encoded by vasa and has extensive sequence similarity to ATP-dependent helicases. Cell *55*, 577–587.

Jankowsky, E., Gross, C.H., Shuman, S., and Pyle, A.M. (2000). The DExH protein NPH-II is a processive and directional motor for unwinding RNA. Nature *403*, 447–451.

Jankowsky, E., Gross, C.H., Shuman, S., and Pyle, A.M. (2001). Active disruption of an RNA-protein interaction by a DExH/D RNA helicase. Science *291*, 121–125.

Johnson, E.R., and McKay, D.B. (1999). Crystallographic structure of the amino terminal domain of yeast initiation factor 4A, a representative DEAD-box RNA helicase. RNA *5*, 1526–1534.

Johnstone, O., and Lasko, P. (2004). Interaction with eIF5B is essential for Vasa function during development. Development *131*, 4167–4178.

Jones, T.A., Zou, J.-Y., Cowan, S.W., and Kjeldgaard, M. (1991). Improved methods for building protein models in electron density maps and the location of errors in these models. Acta Crystallogr. A *47*, 110–119.

Kurimoto, K., Muto, Y., Obayashi, N., Terada, T., Shirouzu, M., Yabuki, T., Aoki, M., Seki, E., Matsuda, T., Kigawa, T., et al. (2005). Crystal structure of the N-terminal RecA-like domain of a DEAD-box RNA helicase, the Dugesia japonica vasa-like gene B protein. J. Struct. Biol. *150*, 58–68.

Lasko, P.F., and Ashburner, M. (1988). The product of the Drosophila gene vasa is very similar to eukaryotic initiation factor-4A. Nature *335*, 611–617.

Liang, L., Diehl-Jones, W., and Lasko, P. (1994). Localization of vasa protein to the Drosophila pole plasm is independent of its RNA-binding and helicase activities. Development *120*, 1201–1211.

Linder, P., Lasko, P.F., Ashburner, M., Leroy, P., Nielsen, P.J., Nishi, K., Schnier, J., and Slonimski, P.P. (1989). Birth of the D-E-A-D box. Nature *337*, 121–122.

Lorsch, J.R., and Herschlag, D. (1998). The DEAD box protein eIF4A. 1. A minimal kinetic and thermodynamic framework reveals coupled binding of RNA and nucleotide. Biochemistry *37*, 2180–2193.

Luking, A., Stahl, U., and Schmidt, U. (1998). The protein family of RNA helicases. Crit. Rev. Biochem. Mol. Biol. *33*, 259–296.

Markussen, F.H., Breitwieser, W., and Ephrussi, A. (1997). Efficient translation and phosphorylation of Oskar require Oskar protein and the RNA helicase Vasa. Cold Spring Harb. Symp. Quant. Biol. *62*, 13–17.

Mohr, S., Stryker, J.M., and Lambowitz, A.M. (2002). A DEAD-box protein functions as an ATP-dependent RNA chaperone in group I intron splicing. Cell *109*, 769–779.

Nicol, S.M., and Fuller-Pace, F.V. (1995). The "DEAD box" protein DbpA interacts specifically with the peptidyltransferase center in 23S rRNA. Proc. Natl. Acad. Sci. USA *92*, 11681–11685.

Otwinowski, Z., and Minor, W. (1997). Processing of X-ray diffraction data collected in oscillation mode. Methods Enzymol. *276*, 307–326.

Pang, P.S., Jankowsky, E., Planet, P.J., and Pyle, A.M. (2002). The hepatitis C viral NS3 protein is a processive DNA helicase with cofactor enhanced RNA unwinding. EMBO J. *21*, 1168–1176.

Pause, A., and Sonenberg, N. (1992). Mutational analysis of a DEAD box RNA helicase: the mammalian translation initiation factor eIF-4A. EMBO J. *11*, 2643–2654.

Pause, A., Methot, N., and Sonenberg, N. (1993). The HRIGRXXR region of the DEAD box RNA helicase eukaryotic translation initiation factor 4A is required for RNA binding and ATP hydrolysis. Mol. Cell. Biol. *13*, 6789–6798.

Polach, K.J., and Uhlenbeck, O.C. (2002). Cooperative binding of ATP and RNA substrates to the DEAD/H protein DbpA. Biochemistry *41*, 3693–3702.

Raz, E. (2000). The function and regulation of vasa-like genes in germ-cell development. Genome Biol. *1*, REVIEWS1017. Published online September 1, 2000. 10.1186/gb-2000-1-3-reviews1017.

Rocak, S., and Linder, P. (2004). DEAD-box proteins: the driving forces behind RNA metabolism. Nat. Rev. Mol. Cell Biol. *5*, 232–241.

Rogers, G.W., Jr., Richter, N.J., and Merrick, W.C. (1999). Biochemical and kinetic characterization of the RNA helicase activity of eukaryotic initiation factor 4A. J. Biol. Chem. *274*, 12236–12244.

Rogers, G.W., Jr., Lima, W.F., and Merrick, W.C. (2001). Further characterization of the helicase activity of eIF4A. Substrate specificity. J. Biol. Chem. *276*, 12598–12608.

Rorth, P. (1998). Gal4 in the Drosophila female germline. Mech. Dev. *78*, 113–118.

Rozen, F., Edery, I., Meerovitch, K., Dever, T.E., Merrick, W.C., and Sonenberg, N. (1990). Bidirectional RNA helicase activity of eucaryotic translation initiation factors 4A and 4F. Mol. Cell. Biol. *10*, 1134–1144.

Scheffzek, K., Ahmadian, M.R., Kabsch, W., Wiesmuller, L., Lautwein, A., Schmitz, F., and Wittinghofer, A. (1997). The Ras-RasGAP complex: structural basis for GTPase activation and its loss in oncogenic Ras mutants. Science *277*, 333–338.

Sengoku, T., Nureki, O., Dohmae, N., Nakamura, A., and Yokoyama, S. (2004). Crystallization and preliminary X-ray analysis of the helicase domains of Vasa complexed with RNA and an ATP analogue. Acta Crystallogr. D Biol. Crystallogr. *60*, 320–322.

Shi, H., Cordin, O., Minder, C.M., Linder, P., and Xu, R.M. (2004). Crystal structure of the human ATP-dependent splicing and export factor UAP56. Proc. Natl. Acad. Sci. USA *101*, 17628–17633.

Silverman, E., Edwalds-Gilbert, G., and Lin, R.J. (2003). DExD/H-box proteins and their partners: helping RNA helicases unwind. Gene *312*, 1–16.

Singleton, M.R., and Wigley, D.B. (2002). Modularity and specialization in superfamily 1 and 2 helicases. J. Bacteriol. *184*, 1819–1826.

Story, R.M., Li, H., and Abelson, J.N. (2001). Crystal structure of a DEAD box protein from the hyperthermophile Methanococcus jannaschii. Proc. Natl. Acad. Sci. USA *98*, 1465–1470.

Styhler, S., Nakamura, A., Swan, A., Suter, B., and Lasko, P. (1998). vasa is required for GURKEN accumulation in the oocyte, and is involved in oocyte differentiation and germline cyst development. Development *125*, 1569–1578.

Svitkin, Y.V., Pause, A., Haghighat, A., Pyronnet, S., Witherell, G., Belsham, G.J., and Sonenberg, N. (2001). The requirement for eukaryotic initiation factor 4A (eIF4A) in translation is in direct proportion to the degree of mRNA 5′ secondary structure. RNA *7*, 382–394.

Tanner, N.K., Cordin, O., Banroques, J., Doere, M., and Linder, P. (2003). The Q motif: a newly identified motif in DEAD box helicases may regulate ATP binding and hydrolysis. Mol. Cell *11*, 127–138.

Terwilliger, T.C., and Berendzen, J. (1999). Automated MAD and MIR structure solution. Acta Crystallogr. D Biol. Crystallogr. *55*, 849–861.

Thompson, J.D., Higgins, D.G., and Gibson, T.J. (1994). CLUSTAL W: improving the sensitivity of progressive multiple sequence alignment through sequence weighting, position-specific gap penalties and weight matrix choice. Nucleic Acids Res. *22*, 4673–4680.

Tinker, R., Silver, D., and Montell, D.J. (1998). Requirement for the vasa RNA helicase in gurken mRNA localization. Dev. Biol. *199*, 1–10.

Tomancak, P., Guichet, A., Zavorszky, P., and Ephrussi, A. (1998). Oocyte polarity depends on regulation of gurken by Vasa. Development *125*, 1723–1732.

Weeks, C.M., and Miller, R. (1999). The design and implementation of SnB v2.0. J. Appl. Crystallogr. *32*, 120–124.

Zhao, R., Shen, J., Green, M.R., MacMorris, M., and Blumenthal, T. (2004). Crystal structure of UAP56, a DExD/H-box protein involved in pre-mRNA splicing and mRNA export. Structure *12*, 1373–1381.

Accession Numbers

Coordinates and structure factors have been deposited in the Protein Data Bank with the ID code 2DB3.